Hindawi Publishing Corporation
Journal of Nanomaterials
Volume 2013, Article ID 517648, 8 pages
http://dx.doi.org/10.1155/2013/517648

Research Article

Heterogeneous Deposition of Cu_2O Nanoparticles on TiO_2 Nanotube Array Films in Organic Solvent

Xinwen Huang[1,2] and Zongjian Liu[1]

[1] *Resource & Environment Catalysis Institute, College of Chemical Engineering and Materials Science, Zhejiang University of Technology, Hangzhou 300014, China*
[2] *College of Biological and Environmental Engineering, Zhejiang University of Technology, Hangzhou 300014, China*

Correspondence should be addressed to Zongjian Liu; zjliu@zjut.edu.cn

Received 27 June 2013; Accepted 26 July 2013

Academic Editor: Guangyu Zhao

Copyright © 2013 X. Huang and Z. Liu. This is an open access article distributed under the Creative Commons Attribution License, which permits unrestricted use, distribution, and reproduction in any medium, provided the original work is properly cited.

A novel method for decoration of anodic TiO_2 nanotube array films (NAFs) with Cu_2O nanoparticles has been reported. The method is based on the reduction of Cu(II) in a mixture of ethylene glycol and N,N-dimethylformamide at 120°C for 16 h, where the resulting Cu_2O can heterogeneously nucleate and grow on TiO_2 NAFs. The nanosized Cu_2O is found to be well dispersed on the wall of TiO_2 nanotubes without blocking the nanotube, a commonly observed phenomenon in the case of deposition of Cu_2O via electrochemical method. The amount of Cu_2O deposited on the TiO_2 NAFs can be varied by adjusting the concentration of Cu(II) in the organic solution. UV-vis spectra measurement indicates that the decoration of TiO_2 NAFs with Cu_2O nanoparticles greatly improves their ability to respond to visible light. By examining the photocurrent and photodegradation of methyl orange under simulated sunlight, it is found that these Cu_2O-decorated TiO_2 NAFs show much more photoactive in comparison with the as-prepared TiO_2 NAFs.

1. Introduction

Because of their large aspect ratio and high specific surface area, materials with one-dimensional (1D) structures, for example, nanotubes and nanowires, often exhibit different performances compared to the bulk counterparts. The unique properties of these 1D nanostructures have shown potential applications in many fields, such as electronics, catalysis, data storage, optics, and sensors [1–3]. 1D TiO_2 nanostructures are of great scientific and technical interest because they exhibit excellent photocatalytic activities [4–7]. Over the past decade, great attention has been paid into the synthesis and application of TiO_2 nanotube arrays prepared by anodic oxidation of Ti metal in F^--containing solutions [7–11]. The highly ordered nanotube arrays not only possess high surface area, but also provide an efficient transport channel for photogenerated electrons [12]. Furthermore, unlike the powder-typed TiO_2 photocatalysts which often need be immobilized onto solid substrates for practical application [13, 14], the TiO_2 nanotube arrays are grown on Ti substrates and thus the formed TiO_2 nanotube array films (NAFs) can be directly used as photoanodes for photoinduced redox reactions such as water splitting [15] and decomposition of harmful compounds [7].

However, TiO_2 nanotube arrays possess a wide band gap (~3.2 eV) and thus only respond well to ultraviolet light, which is a great hindrance to their use under sunlight. To extend their light-response scope from ultraviolet to visible light region, a common approach is postdecoration of TiO_2 NAFs with narrow band gap semiconductors, for example, Cu_2O [16–20], Fe_2O_3 [21] and CdS [22]. When TiO_2 NAFs are decorated with Cu_2O, a p-type semiconductor with a direct band gap of ~2.2 eV, electrons excited under visible light may transfer from the conduction band of Cu_2O to that of TiO_2 since the conduction band (CB) edge for Cu_2O is much higher than that of TiO_2 [23]. As a result, the recombination probability of the photoexcited electrons and holes will be reduced, leading to a great improvement in photocatalytic activity. So far, the methods for the decoration

of TiO_2 nanotube arrays with Cu_2O mainly include electrodeposition [16–18], sonoelectrochemical deposition [19], and photocatalytic reduction [20]. In the present work, we report a new method for loading of Cu_2O nanoparticles onto TiO_2 NAFs. The method is based on the reduction of Cu (II) in a mixture of ethylene glycol (EG) and N,N-dimethylformamide (DMF), where the resulting Cu_2O can heterogeneously nucleate and grow on TiO_2 NAFs. In comparison with commonly used electrodeposition (including sonoelectrochemical deposition), the size of Cu_2O is small, and the nanosized Cu_2O is well dispersed on the wall of TiO_2 nanotubes without blocking the nanotube.

2. Experimental Details

2.1. Synthesis of the Films. Ti foils were cut into pieces (7.2 cm × 1.7 cm × 0.4 mm), polished with abrasive paper, and then washed with deionized water. The polished Ti pieces were degreased in a mixed solution of NaOH and Na_2CO_3 (the ratio of $NaOH : Na_2CO_3 : H_2O$ by weight is 5 : 2 : 100, resp.) at 85°C for 1.5 h, and then washed with deionized water. Before anodic oxidization, one side of the pretreated Ti piece was sealed with epoxy resin, and then etched in a 10 wt% HF aqueous solution at room temperature for about 20 s, followed by washing with deionized water. The anodic oxidization of the Ti piece was conducted in an EG solution containing KF (0.7 wt%) and H_2O (1.8 wt%) at ~25°C, where a Cu plate was used as cathode and a constant voltage of 50 V was applied between two electrodes. The anodic oxide layer was formed by a three-step method. Firstly, the Ti piece was anodized for 2 h, and then the grown oxide layer was removed by an adhesive tape. Secondly, the above procedure was repeated. Finally, the Ti piece was reanodized under the same conditions for 1 h. After anodization, the sample was washed thoroughly with deionized water and then dried in the oven at 40°C for about 12 h.

Deposition of Cu_2O on TiO_2 NAFs was conducted in a 50 mL Teflon-lined autoclave. The autoclave was filled with a solution containing 30 mL of EG and 10 mL of DMF, where a certain amount of $CuSO_4$ (ranging from 0.005 to 0.05 g) was previously dissolved. The as-prepared TiO_2 NAFs were immersed in the organic solution, and then the sealed autoclave was kept in an oven at 120°C for 16 h. After the autoclave was cooled down to room temperature naturally, the resulting samples were removed from the organic solution, washed several times with deionized water, and subsequently dried in an oven at 40°C for about 12 h.

2.2. Characterization and Photocatalytic Activity Evaluation of the Films. The surface morphology of the films was examined using a scanning electron microscope (SEM, Hitachi S-4700) operating at 15 kV. X-ray diffraction (XRD) analysis was performed on a Thermo ARL XTRA X-ray diffractometer using Cu Kα X-ray source. The chemical composition of the as-prepared film was characterized by an energy-dispersive X-ray spectrometer (EDS) attached to SEM operating at 15 kV. The ultraviolet-visible (UV-vis) diffuse reflectance spectra were recorded on a UV-2550 (SHIMADSU) spectrophotometer with $BaSO_4$ as the reference. The photoelectrochemical property of the film electrodes was evaluated in a three-electrode cell using a Pt wire as counter electrode and a saturated calomel electrode (SCE) as reference electrodes. If needed, the working electrode could be irradiated from the front side by a sunlight-simulation lamp (Osram Ultra Vitalux 300W). The current with or without irradiation was measured in a 0.25 M Na_2SO_4 aqueous solution using a potentiostat (CHI 620B, CHI Co.). Photocatalytic activities of the samples were evaluated by the photodegradation of methyl orange (MO) solution with an initial concentration of 5.0 mg/L under simulated sunlight. The photodegradation experiments were conducted in a quartz reactor. In each test, one piece of the sample was hung in the liquid. Prior to irradiation, the suspension was kept in the dark for 60 min to achieve the adsorption-desorption equilibrium between the photocatalyst and methyl orange. Then, the solution was exposed to the light irradiation, and samples were taken at given time interval to analyze the concentration of MO by measuring the absorbance with the spectrophotometer.

3. Results and Discussion

To decorate TiO_2 NAFs with nanosized Cu_2O, a suitable condition for reduction of Cu^{2+} in organic solvent should be chosen. Figure 1(a) shows the XRD patterns of the products obtained by reduction of Cu^{2+} (2 mmol) in a mixture of EG and DMF at different temperatures. At a temperature of 120°C, all the diffraction peaks appearing in the XRD pattern of the product (indicated by the solid circles) can be indexed to cubic Cu_2O phase (JCPDS number 65-3288), at which the peaks at 2θ values of 29.6°, 36.5°, 42.4°, and 61.5° correspond to 110, 111, 200, and 220 lattice planes of Cu_2O, respectively. The broaden peaks indicate that the size of Cu_2O is very small. The average crystal size calculated by Scherrer's equation for (111) reflections of Cu_2O is about 10 nm. The SEM image shown in Figure 1(b) reveals that these small-sized Cu_2O nanocrystals are severely aggregated as a result of reduction in surface energy. When the reduction is conducted at 140°C, we can observe two new peaks at 2θ of 43.2° and 50.4° (indicated by open circles), which can be, respectively, assigned to the diffraction of (111) and (200) planes of cubic Cu (JCPDS number 04-0836). The result indicates the formation of Cu at 140°C. As the temperature is raised to 160°C, all the diffraction peaks of Cu_2O disappear. Moreover, the peaks assigned to Cu become very sharp, suggesting that the growth of Cu crystals of large size occurs. This is confirmed by the SEM image of this sample (see Figure 1(c)), where Cu microcrystals can be observed. Therefore, we chose a temperature of 120°C to deposit Cu_2O on TiO_2 nanotube arrays, where the concentration of Cu^{2+} in the mixture of EG and DMF is changed to control the amount of Cu_2O deposited on the films.

Figure 2(a) presents the digital photos of TiO_2 NAFsbefore and after being treated in the mixture of EG and DMF containing different amounts of $CuSO_4$ at 120°C for 16 h. Compared with the untreated TiO_2 film, the treatment in

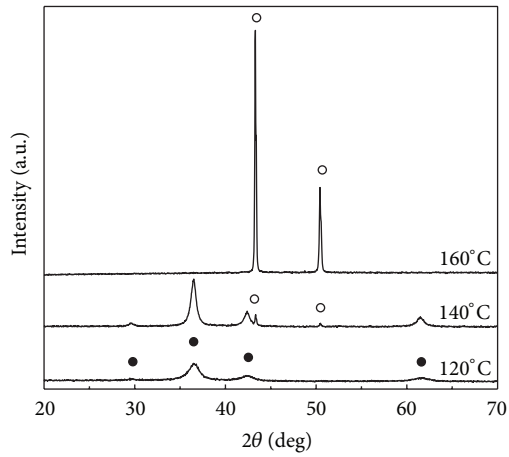

(a)

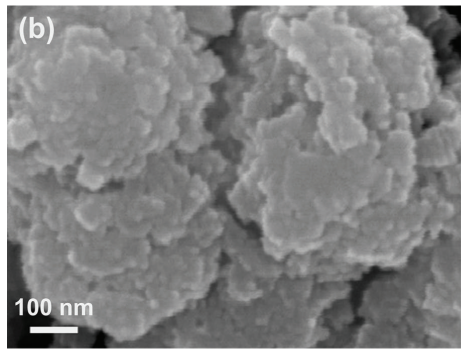

(b)

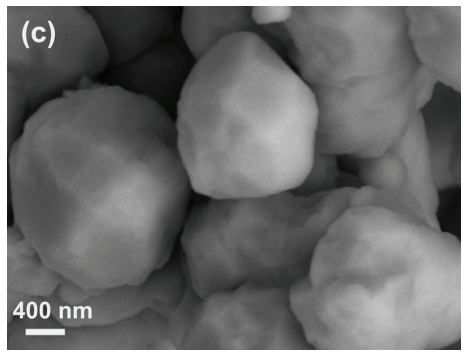

(c)

Figure 1: (a) XRD patterns of the products obtained by reduction of $CuSO_4$ (2 mmol) in a mixture of EG and DMF at different temperatures. (b) and (c) are the corresponding SEM images of the products obtained at 120°C and 160°C, respectively.

$CuSO_4$-contianing organic solution can result in an obvious color change, and the color of the treated TiO_2 NAFs changes from light yellow to dull red as the amount of $CuSO_4$ in the organic solution increases. These results hint that the deposition of Cu_2O on the TiO_2 NAFs occurs after treatment in $CuSO_4$-contianing organic solutions, especially when the amount of $CuSO_4$ is high. The XRD patterns of

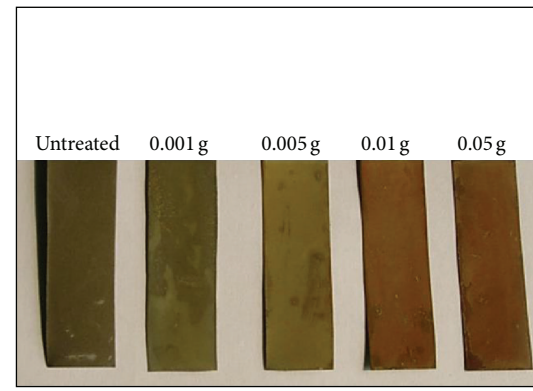

(a)

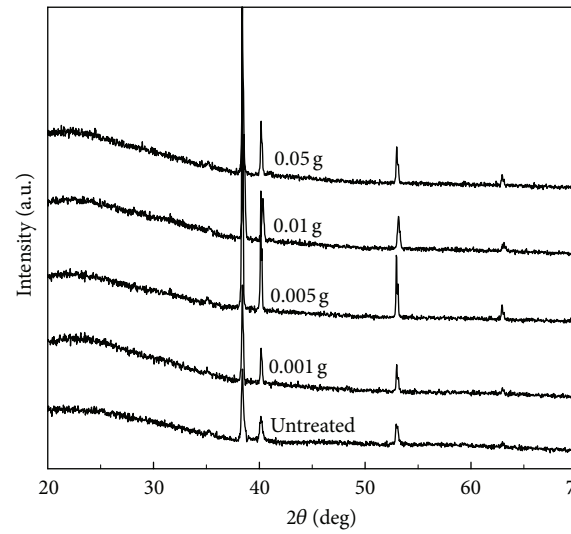

(b)

Figure 2: (a) Digital photos and (b) XRD patterns of TiO_2 NAFs before and after treatment in the mixture of EG and DMF containing different amounts of $CuSO_4$ at 120°C for 16 h.

these untreated and treated TiO_2 NAFs films are shown in Figure 2(b). In the XRD pattern of the untreated TiO_2 film, the peaks at 35.1°, 38.4°, 40.2°, 53.0°, and 63.0° can be attributed to the background of Ti (JCPDS 44-1294). These peaks correspond to the diffraction of (100), (002), (101), (102), and (110) lattice planes of Ti, respectively. No diffraction peak attributed to TiO_2 phase can be observed, indicating that the TiO_2 nanotube arrays are amorphous. After being treated in $CuSO_4$-contianing organic solutions at 120°C for 16 h, the TiO_2 nanotube arrays are still in the amorphous state. In addition, in the XRD patterns of all treated NAFs we cannot observe any diffraction peak which can be assigned to the Cu_2O phase, indicating that Cu_2O might be well-dispersed on TiO_2 NAFs.

The chemical composition of TiO_2 NAFs before and after being treated in $CuSO_4$-containing organic solution was characterized by EDS. Figure 3(a) shows the EDS spectra of these films, and the amount of Cu calculated from the spectra is presented in Figure 3(b) (see open circles). It is obvious that a small amount of fluorine is incorporated into

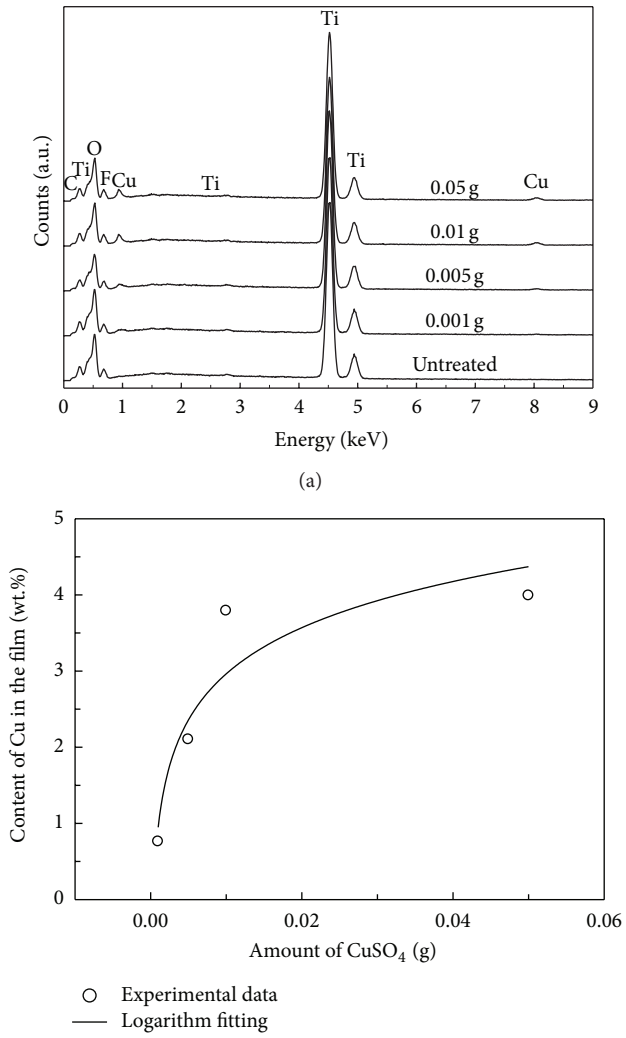

Figure 3: (a) EDS spectra of TiO_2 NAFs before and after treatment in the mixture of EG and DMF containing different amounts of $CuSO_4$ at 120°C for 16 h; (b) plot of content of Cu in the film against the amount of $CuSO_4$ in the solution (see open circles). The curve is the fitting result using a logarithm equation of $y = a + b\ln x$.

TiO_2 nanotubes, and treatment in $CuSO_4$-containing organic solution cannot remove fluorine from the TiO_2 nanotube layer. The observation of fluorine in the nanotube layer should result from the fact that F^- will migrate towards the Ti anode during the anodizing process [24]. From Figure 3(b), we can also find that the amount of Cu in the film shows an increasing trend as the concentration of $CuSO_4$ in the organic solution increases. The increasing trend can be roughly fitted by a logarithm equation of $y = 6.991 + 0.8747\ln x$. The surface morphology of treated TiO_2 NAFs can be found in Figure 4. As can be seen from Figures 4(a) and 4(b), after being treated in organic solution containing a small amount of $CuSO_4$ (viz. 0.001 g and 0.005 g), the amount of Cu_2O decorated on the film (indicated by white arrows) is very small. When the amount of $CuSO_4$ is raised to 0.01 g or 0.05 g (see Figures 4(c) or 4(d)), we can observe many nanoparticles

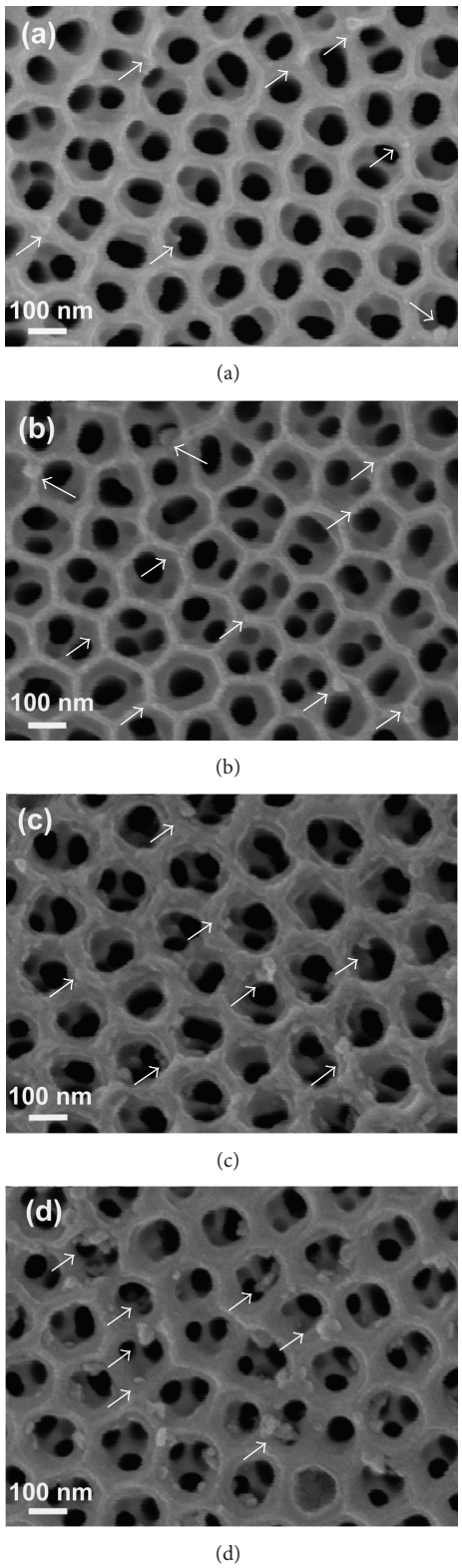

Figure 4: SEM images of TiO_2 NAFs after treatment in the mixture of EG and DMF containing different amounts of $CuSO_4$ at 120°C for 16 h: (a) 0.001 g, (b) 0.005 g, (c) 0.01 g, and (d) 0.05 g.

deposited on the films (indicated by white arrows). These nanosized Cu_2O particles are well dispersed on the wall of

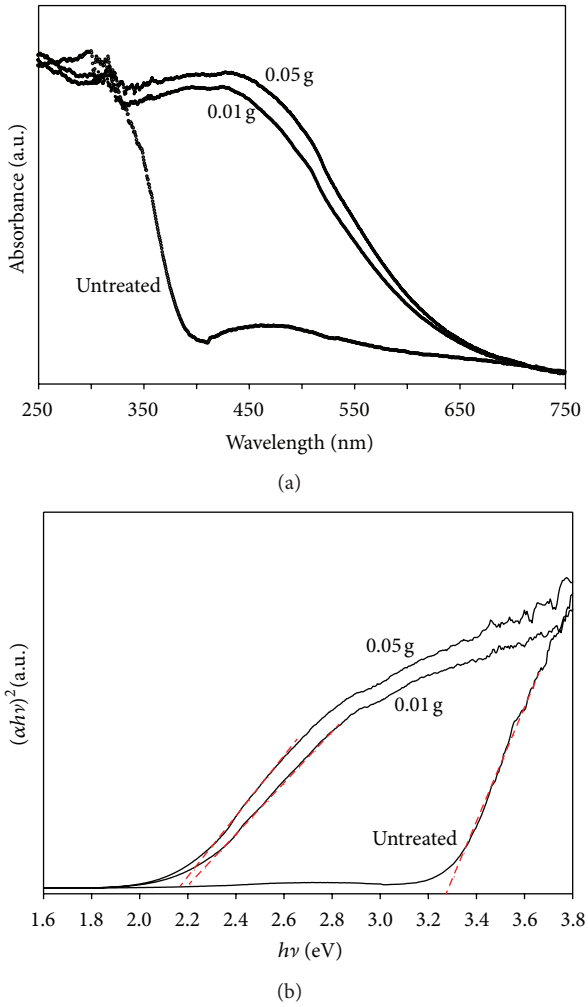

FIGURE 5: (a) UV-vis diffuse reflectance spectrum of TiO_2 NAFs before and after treatment in the mixture of EG and DMF containing 0.01 or 0.05 g $CuSO_4$ at 120°C for 16 h; (b) plot of $(\alpha h\nu)^2$ against photon energy ($h\nu$) for these three TiO_2 NAFs.

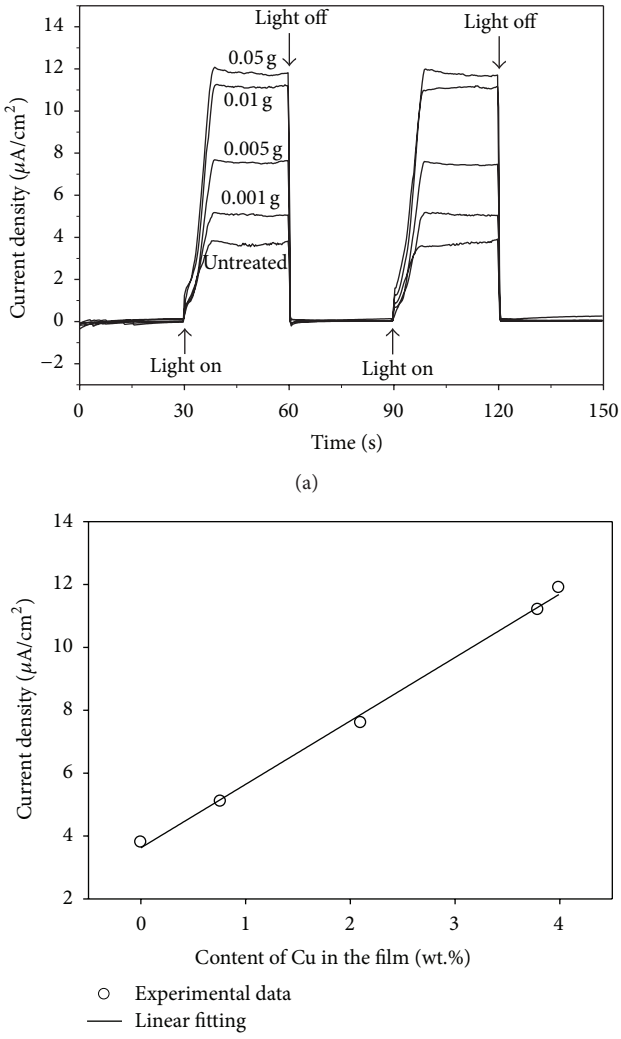

FIGURE 6: (a) Measured photocurrent density of TiO_2 NAFs before and after treatment in the mixture of EG and DMF containing different amounts of $CuSO_4$ at 120°C for 16 h; (b) plot of photocurrent density against the amount of Cu in the film.

TiO_2 nanotubes without blocking the nanotube, a commonly observed phenomenon in the case of deposition of Cu_2O via electrochemical method [16–19]. The observed result might be related to the fact that in the case of electrodeposition the applied voltage favors the formation of Cu_2O crystals of large size [16–19], which may easily block the nanotube, while in our case the growth of Cu_2O resulting from the reduction of Cu(II) in organic solvent tends to form Cu_2O nanocrystals (see Figure 1(a)). In addition, when Cu_2O heterogeneously deposits on TiO_2 NAFs, the interaction between Cu_2O and TiO_2 can reduce the surface energy of Cu_2O nanocrystals and thus reduces their aggregation degree (namely, very large particles as observed in Figure 1(b) are not formed by aggregation of Cu_2O nanocrystals). As a result, the nanotubes are not easily blocked by these small-sized Cu_2O particles. Despite the observation of Cu_2O nanoparticles on the film surface, however, these Cu_2O nanoparticles cannot be detected by XRD (see Figure 2(b)). The possible reason for this is that these Cu_2O nanoparticles are distributed on the film surface. Compared with the corresponding powder materials, nanosized materials dispersed on the film surface is often more difficult to be detected by conventional XRD technique when their crystal size or amount is not large enough. In addition, since the small-sized Cu_2O particles tend to aggregate due to high surface energy (see Figure 1(b)), the particles of large size observed in Figure 4 might also be composed of several small-sized particles, which further make it difficult to detect Cu_2O phase by XRD.

To determine whether the treatment of TiO_2 NAFs in $CuSO_4$-containing organic solution can extend their light-response scope from ultraviolet to visible light region, we have measured the UV-vis diffuse reflectance spectrum of the TiO_2 NAFs treated in organic solution containing relatively high amount of $CuSO_4$ (viz. 0.01 g and 0.05 g). Figure 5(a) shows the UV-vis diffuse reflectance spectrum of these two

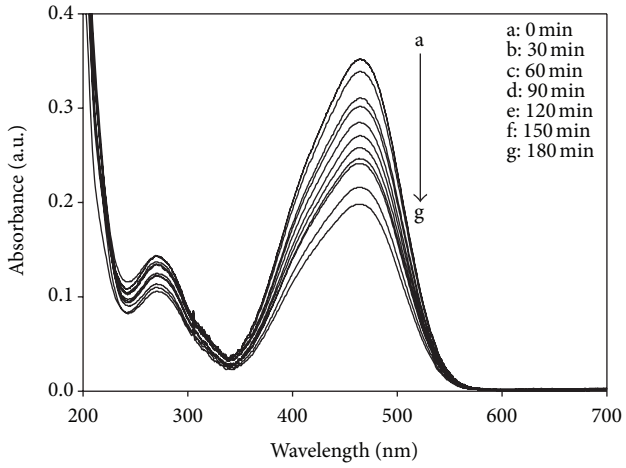

Figure 7: Comparison of the temporal evolution of the adsorption spectra of MO solution degraded by two TiO_2 NAFs: (a) untreated and (b) after treatment in the mixture of EG and DMF containing 0.05 g $CuSO_4$ at 120°C for 16 h.

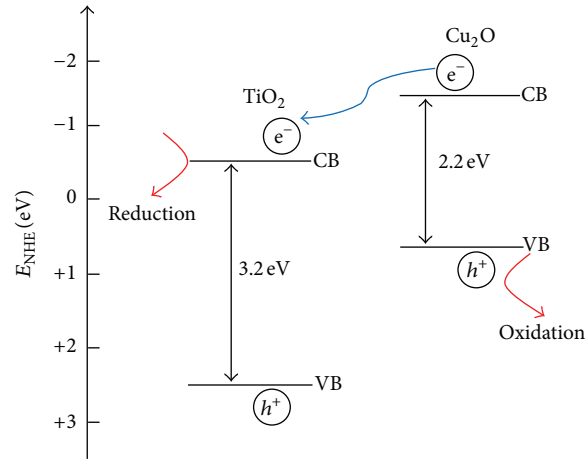

Figure 8: Schematic diagram for describing the band gap and electron transfer for the Cu_2O/TiO_2 system. CB, VB, and NHE are the abbreviations of conduction band, valance band, and normal hydrogen electrode, respectively.

treated TiO_2 NAFs. For comparison, the UV-vis diffuse reflectance spectrum of the untreated film is also shown. Compared with the untreated film, both two treated TiO_2 NAFs exhibit significant increases in photoadsorption at the wavelength larger than 400 nm, suggesting that they can respond well to visible light. The absorption coefficient α follows the equation $\alpha h\nu = A(h\nu - E_g)^{\gamma}$, where h, ν, A, E_g, and γ are, respectively, plank constant, light frequency, proportionality coefficient that depends on the properties of the material, band gap, and a constant that can take different values depending on the type of electronic transition [25]. For a permitted direct transition, $\gamma = 0.5$. Figure 5(b) shows the plot of $(\alpha h\nu)^2$ against $h\nu$ for three films, where the value of E_g is obtained by extrapolating the linear part of the graphics to the axis of the abscissa (see dashed red lines). The band gaps estimated from the plots of $(\alpha h\nu)^2$ verses photon energy ($h\nu$) are about 3.27, 2.20, and 2.16 eV for untreated TiO_2 NAF and two treated TiO_2 NAFs, respectively, (see Figure 5(b)).

The observed decrease in the band gap after treatment in $CuSO_4$-containing organic solutions is in line with the UV-vis adsorption spectra with a red shift. Since the band gap of Cu_2O is about 2.2 eV, the value of 2.20 and 2.16 eV obtained for two treated NAFs confirms that Cu_2O is deposited on TiO_2 NAF.

The photoelectrochemical property of the as-prepared or Cu_2O-decorated TiO_2 film electrodes is investigated by measuring the anodic photocurrent in a 0.25 M Na_2SO_4 aqueous solution. As can be seen from Figure 6(a), without light irradiation (from 0–30 s), the dark currents for all films are almost equal to zero. When the light is on (from 30 to 60 s), the photocurrent increases sharply till reaching a certain value. If the light is off (from 60 to 90 s), the photocurrent declines rapidly to about zero. A similar phenomenon can also be observed in the range of 90–150 s. The observed photocurrent represents the anodic oxidation of water to oxygen by the photogenerated holes at the film electrode under light irradiation. For the untreated TiO_2 film, under light irradiation the electrons are excited from the valence band to conduction band of TiO_2 to form photogenerated electron-hole pairs. The photogenerated electrons and holes are separated under the external potential bias, and most electrons are transferred to titanium substrate to produce photocurrent with the hole oxidizing water to oxygen on the surface of the anode. It is clear from Figure 6(a) that the decoration of Cu_2O can lead to a great rise in photocurrent density, where the photocurrent density for the treated TiO_2 NAF in organic solution containing 0.05 g $CuSO_4$ is about 3 times higher than that for the untreated TiO_2 NAF. It is also interesting to note that the photocurrent density almost increases linearly with the amount of Cu in the film (see Figure 6(b)). These results suggest that the decoration of Cu_2O can greatly improve the water splitting performance of the TiO_2 NAFs under sunlight. The comparison of photocatalytic activity between untreated and treated TiO_2 NAFs in organic solution containing 0.05 g $CuSO_4$ is also evaluated

by the photodegradation of MO. The MO aqueous solution shows an intense absorption band centered at ~464 nm and the peak intensity is proportional to its concentration. Figure 7 shows a comparison of the temporal evolution of the adsorption spectra of MO solution degraded by two films. It is obvious that the Cu_2O-decorated TiO_2 NAF exhibits better photocatalytic activity than the undecorated one. The degradation efficiency of MO for the Cu_2O-decorated film reaches ~54.7% in 3 h, while that for the undecorated film is ~31.2%.

The enhanced activity of the Cu_2O-decorated NAFs observed in our experiments can be attributed to the combined effect of several factors. Firstly, under simulated sunlight, TiO_2 can be excited by UV light, and Cu_2O can be excited by visible light, which will generate more electrons and holes for photocatalytic reactions as compared to undecorated TiO_2 NAF. Secondly, the combination of TiO_2 with Cu_2O will lead to a reduced recombination of the photoexcited electrons and holes due to the difference between the band edges of Cu_2O and TiO_2 semiconductors. As shown in Figure 8, the electron excited under visible light may transfer from the conduction band of Cu_2O to that of TiO_2 since the conduction band edge for Cu_2O is higher than that of TiO_2 [23]. As a result, the recombination probability of the photoexcited electrons and holes will be reduced, leading to an improvement in photocatalytic activity.

4. Conclusions

In summary, we have presented a novel method for modification of anodic TiO_2 nanotube array films with Cu_2O nanoparticles. The method is based on the theory of heterogeneous nucleation and growth in an organic solvent (ethylene glycol and N,N-dimethylformamide) containing $CuSO_4$. The Cu_2O nanoparticles are found to be well dispersed on the wall of TiO_2 nanotubes without blocking the nanotube, and the amount of Cu_2O deposited on the TiO_2 nanotube array films shows an increasing trend as the concentration of $CuSO_4$ increases. The decorated nanotube array films can respond well to both ultraviolet and visible light and show much better photocatalytic activity than the undecorated film.

Acknowledgment

This work was supported by the Natural Science Foundation of Zhejiang Province (no. LY12B07011).

References

[1] Y. Xia, P. Yang, Y. Sun et al., "One-dimensional nanostructures: synthesis, characterization, and applications," *Advanced Materials*, vol. 15, no. 5, pp. 353–389, 2003.

[2] W. Zhou, H. Liu, R. I. Boughton et al., "One-dimensional single-crystalline Ti-O based nanostructures: properties, synthesis, modifications and applications," *Journal of Materials Chemistry*, vol. 20, no. 29, pp. 5993–6008, 2010.

[3] J. Pan, H. Shen, and S. Mathur, "One-dimensional SnO_2 nanostructures: synthesis and applications," *Journal of Nanotechnology*, vol. 2012, Article ID 917320, 12 pages, 2012.

[4] J. Qu and C. Lai, "One-dimensional TiO_2 nanostructures as photoanodes for dye-sensitized solar cells," *Journal of Nanomaterials*, vol. 2013, Article ID 762730, 11 pages, 2013.

[5] S. Wang, T. Wang, Y. W. Ding et al., "Gas-supported high-photoactivity TiO_2 nanotubes," *Journal of Nanomaterials*, vol. 2012, Article ID 909473, 6 pages, 2012.

[6] J. Jitputti, Y. Suzuki, and S. Yoshikawa, "Synthesis of TiO_2 nanowires and their photocatalytic activity for hydrogen evolution," *Catalysis Communications*, vol. 9, no. 6, pp. 1265–1271, 2008.

[7] Q. Zhang, H. Xu, and W. Yan, "Highly ordered TiO_2 nanotube arrays: recent advances in fabrication and environmental applications—a review," *Nanoscience and Nanotechnology Letters*, vol. 4, no. 5, pp. 505–519, 2012.

[8] K. M. Kummer, E. Taylor, and T. J. Webster, "Biological applications of anodized TiO_2 nanostructures: a review from orthopedic to stent applications," *Nanoscience and Nanotechnology Letters*, vol. 4, no. 5, pp. 83–493, 2012.

[9] Y. Ku, Y.-S. Chen, W.-M. Hou, and Y.-C. Chou, "Effect of NH_4F concentration in electrolyte on the fabrication of TiO_2 nanotube arrays prepared by anodisation," *Micro & Nano Letters*, vol. 7, no. 9, pp. 939–942, 2012.

[10] Z. C. Xu, Q. Li, S. A. Gao, and J. K. Shang, "Synthesis and characterization of niobium-doped TiO_2 nanotube arrays by anodization of Ti-20Nb alloys," *Journal of Materials Science & Technology*, vol. 28, no. 10, pp. 865–870, 2012.

[11] C. A. Grimes, "Synthesis and application of highly ordered arrays of TiO_2 nanotubes," *Journal of Materials Chemistry*, vol. 17, no. 15, pp. 1451–1457, 2007.

[12] M. Paulose, K. Shankar, O. K. Varghese, G. K. Mor, and C. A. Grimes, "Application of highly-ordered TiO_2 nanotube-arrays in heterojunction dye-sensitized solar cells," *Journal of Physics D*, vol. 39, no. 12, pp. 2498–2503, 2006.

[13] S. Mozia, P. Brozek, J. Przepiorski, B. Tryba, and A. W. Morawski, "Immobilized TiO_2 for phenol degradation in a pilot-scale photocatalytic reactor," *Journal of Nanomaterials*, vol. 2012, Article ID 949764, 10 pages, 2012.

[14] W. Y. Zhao, W. Y. Fu, H. B. Yang et al., "Synthesis and photocatalytic activity of Fe-doped TiO_2 supported on hollow glass microbeads," *Nano-Micro Letters*, vol. 3, no. 1, pp. 20–24, 2011.

[15] C. W. Lai and S. Sreekantan, "TiO_2 nanotubes arrays: improved photoelectrochemical water splitting by adding pptimum amount of ethylene glycol in KOH Electrolyte," *Nanoscience and Nanotechnology Letters*, vol. 5, no. 1, pp. 57–62, 2013.

[16] S. Zhang, S. Zhang, F. Peng, H. Zhang, H. Liu, and H. Zhao, "Electrodeposition of polyhedral Cu_2O on TiO_2 nanotube arrays for enhancing visible light photocatalytic performance," *Electrochemistry Communications*, vol. 13, no. 8, pp. 861–864, 2011.

[17] S. S. Zhang, C. Liu, X. L. Liu et al., "Nanocrystal Cu_2O-loaded TiO_2 nanotube array films as high-performance visible-light bactericidal photocatalyst," *Applied Microbiology and Biotechnology*, vol. 96, no. 5, pp. 1201–1207, 2012.

[18] L. Huang, S. Zhang, F. Peng et al., "Electrodeposition preparation of octahedral-Cu_2O-loaded TiO_2 nanotube arrays for visible light-driven photocatalysis," *Scripta Materialia*, vol. 63, no. 2, pp. 159–161, 2010.

[19] Y. B. Liu, H. B. Zhou, J. H. Li et al., "Enhanced photoelectrochemical properties of Cu_2O-Loaded Short TiO_2 nanotube array electrode prepared by sonoelectrochemical deposition," *Nano-Micro Letters*, vol. 2, no. 4, pp. 277–284, 2010.

[20] Y. Hou, X. Y. Li, Q. D. Zhao, X. Quan, and G. H. Chen, "Fabrication of Cu_2O/TiO_2 nanotube heterojunction arrays and investigation of its photoelectrochemical behavior," *Applied Physics Letters*, vol. 95, no. 9, Article ID 093108, 2009.

[21] Y. Q. Cong, Z. Li, Q. Wang, Y. Zhang, Q. Xu, and F. X. Fu, "Enhanced photoeletrocatalytic activity of TiO_2 nanotube arrays modified with simple transition metal oxides (Fe_2O_3, CuO, NiO)," *Acta Physico-Chimica Sinica*, vol. 28, no. 6, pp. 1489–1496, 2012.

[22] G. S. Li, L. Wu, F. Li, P. P. Xu, D. Q. Zhang, and H. X. Li, "Photoelectrocatalytic degradation of organic pollutants via a CdS quantum dots enhanced TiO_2 nanotube arrayelectrode under visible light irradiation," *Nanoscale*, vol. 5, no. 5, pp. 2118–2125, 2013.

[23] M. Ni, M. K. H. Leung, D. Y. C. Leung, and K. Sumathy, "A review and recent developments in photocatalytic water-splitting using TiO_2 for hydrogen production," *Renewable and Sustainable Energy Reviews*, vol. 11, no. 3, pp. 401–425, 2007.

[24] G. D. Sulka, J. Kapusta-Kołodziej, A. Brzózka, and M. Jaskuła, "Fabrication of nanoporous TiO_2 by electrochemical anodization," *Electrochimica Acta*, vol. 55, no. 14, pp. 4359–4367, 2010.

[25] A. Duret and M. Grätzel, "Visible light-induced water oxidation on mesoscopic α-Fe_2O_3 films made by ultrasonic spray pyrolysis," *Journal of Physical Chemistry B*, vol. 109, no. 36, pp. 17184–17191, 2005.

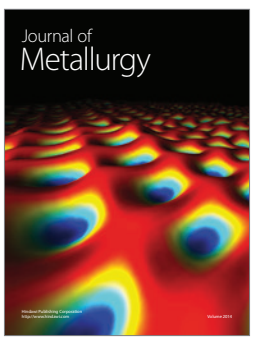

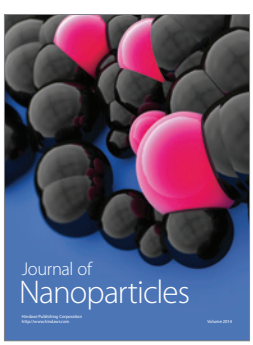

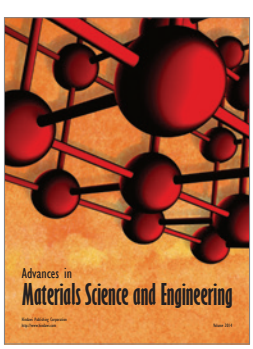

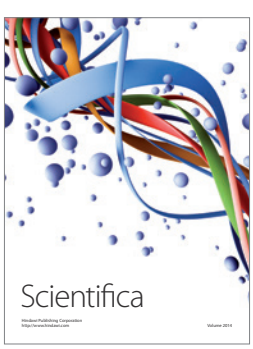

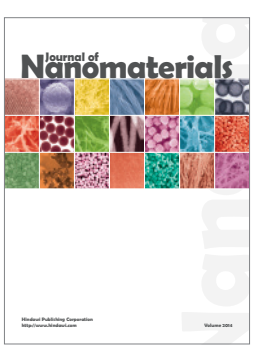

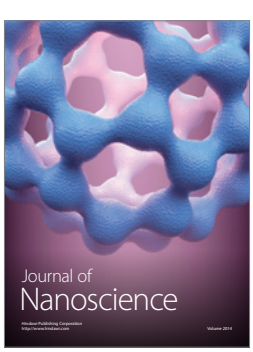

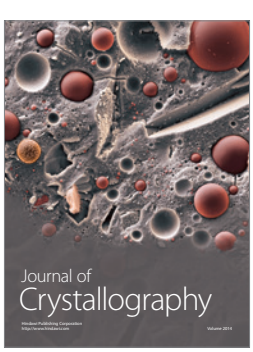

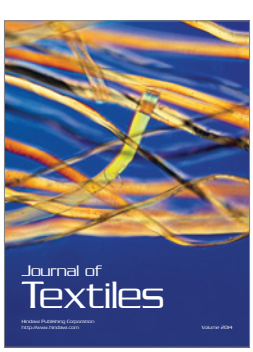

Hindawi

Submit your manuscripts at
http://www.hindawi.com